




# Dopaminergic Projection from Ventral Tegmental Area to Substantia Nigra Pars Reticulata Mediates Chronic Social Defeat Stress–Induced Hypolocomotion

Feng He<sup>1</sup> · Pei Zhang<sup>1,2,3</sup> · Qian Zhang<sup>1</sup> · Guangjian Qi<sup>1</sup> · Hongwei Cai<sup>1</sup> · Tongxia Li<sup>1</sup> · Ming Li<sup>1</sup> · Jiazhen Lu<sup>1</sup> · Jiaen Lin<sup>1</sup> · Jie Ming<sup>4</sup> · Bo Tian<sup>1,2,3</sup> 

Received: 21 May 2021 / Accepted: 4 August 2021 / Published online: 12 August 2021  
© The Author(s), under exclusive licence to Springer Science+Business Media, LLC, part of Springer Nature 2021

## Abstract

Numerous human clinical studies have suggested that decreased locomotor activity is a common symptom of major depressive disorder (MDD), as well as other psychiatric diseases. In MDD, the midbrain ventral tegmental area (VTA) dopamine (DA) neurons are closely related to regulate the information processing of reward, motivation, cognition, and aversion. However, the neural circuit mechanism that underlie the relationship between VTA-DA neurons and MDD-related motor impairments, especially hypolocomotion, is still largely unknown. Herein, we investigate how the VTA-DA neurons contribute to the hypolocomotion performance in chronic social defeat stress (CSDS), a mouse model of depression-relevant neurobehavioral states. The results show that CSDS could affect the spontaneous locomotor activity of mice, but not the grip strength and forced locomotor ability. Chemogenetic activation of VTA-DA neurons alleviated CSDS-induced hypolocomotion. Subsequently, quantitative whole-brain mapping revealed decreased projections from VTA-DA neurons to substantia nigra pars reticulata (SNr) after CSDS treatment. Optogenetic activation of dopaminergic projection from VTA to SNr with the stimulation of phasic firing, but not tonic firing, could significantly increase the locomotor activity of mice. Moreover, chemogenetic activation of VTA-SNr dopaminergic circuit in CSDS mice could also rescued the decline of locomotor activity. Taken together, our data suggest that the VTA-SNr dopaminergic projection mediates CSDS-induced hypolocomotion, which provides a theoretical basis and potential therapeutic target for MDD.

**Keywords** Depression · Hypolocomotion · VTA · SNr · Dopaminergic projection

Feng He and Pei Zhang contributed equally to this work.

✉ Jie Ming  
mingjiewh@126.com

✉ Bo Tian  
tianbo@mails.tjmu.edu.cn

<sup>1</sup> Department of Neurobiology, School of Basic Medicine, Tongji Medical College, Huazhong University of Science and Technology, Wuhan, Hubei Province 430030, People's Republic of China

<sup>2</sup> Institute for Brain Research, Huazhong University of Science and Technology, Wuhan, Hubei Province 430030, People's Republic of China

<sup>3</sup> Key Laboratory of Neurological Diseases, Ministry of Education, Wuhan, Hubei Province 430030, People's Republic of China

<sup>4</sup> Department of Breast and Thyroid Surgery, Union Hospital, Tongji Medical College, Huazhong University of Science and Technology, Wuhan, Hubei Province 430022, People's Republic of China

## Introduction

Major depressive disorder (MDD) is one of the most common mental diseases around the world. It is also a debilitating disease characterized by diverse symptoms, such as depressed mood, anhedonia, appetite or weight changes, sleep difficulties, social impairment, fatigue, and reduction of physical movement [1, 2]. Unfortunately, despite the prevalence of MDD, much of the etiology and, therefore, preventative and treatment measures are still little known. Historically, researchers have employed various forms of chronic stress stimulations to produce behavior adaptations relevant to depression. These include repeated social defeat stress, chronic mild unpredictable stress, foot-shock stress, learned helplessness or chronic restraint stress, followed by anhedonia or despair-like behavior tests in mice [3]. Among the whole outcomes of depression-like behaviors, hypolocomotion is an increasingly major

area of interest within the field of psychiatric research [4]. Hypolocomotion is inhibition of behavior or locomotor activity. It could be measured by locomotor activity test, which could represent a model for vulnerability to stress-induced depression-relevant neurobehavioral states, based on exploratory behavior [5]. Previously published study has also suggested the animal with depression exhibit low rates of locomotor activity [6]. However, the neural basis of hypolocomotion in MDD remains unknown.

In animal models of depression-relevant neurobehavioral states, chronic social defeat stress (CSDS) has proven to be useful in understanding the molecular mechanism and neural basis [7]. Midbrain dopaminergic (DA) neurons, including the ventral tegmental area (VTA)-DA populations, contribute to both the induction and recovery of CSDS-induced depression-like behaviors [8, 9]. Indeed, the VTA area consists of reward-value-coding dopamine neurons [10, 11]. Dopamine-releasing neurons of the VTA play involved in reward-related and goal-directed behaviors, such as positive and negative reinforcement, decision-making, working memory, and aversion [12]. Interestingly, VTA-DA neurons exhibit two patterns of firing in vivo, namely, low-frequency tonic firing and high-frequency phasic firing [13]. The phasic firing of VTA-DA neurons, which is the key mediator in the brain's reward circuit, plays a central role in the mouse model of depression-relevant neurobehavioral states [9, 14]. Moreover, VTA-DA neurons send projections to other brain regions, including NAc, prefrontal cortex (PFC), central amygdala (CeA), basolateral amygdala nucleus (BLA), and hippocampus. Using adeno-associated virus-based anterograde tracing, in conjunction with rabies virus-based trans-synaptic tracing and Cre-based cell-type-specific targeting, the relationships between direct inputs and outputs of VTA-DA neurons have been systematically identified [15]. However, how the outputs of VTA-DA neurons mediate hypolocomotion in MDD remains unclear.

In this study, we have investigated the behavioral adaptations of locomotor activity following CSDS and the role of VTA-DA neurons. We found that CSDS could directly induce hypolocomotion. Using a chemogenetic approach, increased VTA-DA neurons activity significantly reverses the CSDS-induced decline in locomotor activity. To evaluate the change of direct projections from VTA-DA neurons in CSDS mice, whole-brain quantitative mapping is employed, and the result reveals that the neural circuit, from VTA-DA neurons to substantia nigra pars reticulata (SNr), was involved. Optogenetic and chemogenetic activation of VTA-SNr dopaminergic projections could robustly rescue the CSDS-induced hypolocomotion. Collectively, dopaminergic projections from VTA to SNr appear to mediate CSDS-induced hypolocomotion, and this circuit may be involved in MDD.

## Materials and Methods

### Mice

One hundred and sixty 8–12 weeks aged C57BL/6 J male mice and one hundred 4-month-old retired CD1 breeders were purchased from Vital River Laboratory Animal Technology (Beijing, China). The mice were group-housed and maintained at 22–25 °C in a 12-h light/dark cycle (lights on from 8:00 to 20:00 h) with food and water available ad libitum. All animal procedures involving mice were approved by the Institutional Animal Care and Use Committee (IACUC) at Huazhong University of Science and Technology.

### Virus Preparations

Recombinant AAV vectors were used for delivering target genes. AAV9-TH (tyrosine hydroxylase)-Cre, AAV9-DIO-hM3Dq (human M3 muscarinic receptor, Gq)-mCherry, AAV9-DIO-ChR2 (channelrhodopsin-2)-EYFP (enhanced yellow fluorescent protein), AAV2-retro-DIO-ChR2-mCherry, and AAV2-retro-DIO-hM3Dq (Gq)-mCherry were purchased from BrainVTA (BrainVTA Co., Ltd., Wuhan, China). The titer of viruses was as follow: AAV9-TH-Cre,  $7.65 \times 10^{12}$  vg/ml; AAV9-DIO-hM3Dq(Gq)-mCherry,  $2.00 \times 10^{12}$  vg/ml; AAV9-DIO-ChR2-EYFP,  $6.30 \times 10^{12}$  vg/ml; AAV2-retro-DIO-ChR2-mCherry,  $5.99 \times 10^{12}$  vg/ml; AAV2-retro-DIO-hM3Dq(Gq)-mCherry,  $5.13 \times 10^{12}$  vg/mL; and AAV2-retro-DIO-mCherry,  $2.81 \times 10^{12}$  vg/ml. Viral vectors were subdivided into aliquots stored at  $-80$  °C until use.

### Chronic Social Defeat Stress

Chronic social defeat stress (CSDS) was performed according to previously described procedures [7]. Briefly, retired breeder CD1 male mice were screened over three consecutive days and selected for aggressive behavior based on the following criteria: (a) the attack latency under 60 s; (b) attacking for at least two consecutive days. For ten consecutive days, experimental mice were placed into the home cage of a novel CD1 aggressor mouse for 5–10 min, during which they were physically attacked and displayed subordinate posturing. Following the daily defeat, the CD1 and experimental mouse were housed together but separated by a perforated plexiglass partition to allow for visual, olfactory, and auditory contacts, for the remainder of the 24-h period. Control animals were housed in pairs separated by a perforated Plexiglas

partition and changed daily. After the last defeat, all mice were singly housed and tested 24 h later for the battery of behavior tests, including social interaction test, forced swim test, locomotion test, rotarod test, and grip strength test (Fig. 1). And all the mice of CSDS group were included for the above behavior tests.

## Social Interaction and Avoidance

Social avoidance behavior was measured with a novel CD1 mouse in a two-stage social interaction test [7]. In the first 2.5-min “no target” session, test mice were allowed to roam around an open arena (50 cm × 50 cm × 50 cm) with an empty Plexiglas enclosure (10 cm × 6.5 cm × 50 cm) at one end. For the second 2.5-min “target” session, test mice were placed back into the arena with an unfamiliar CD1

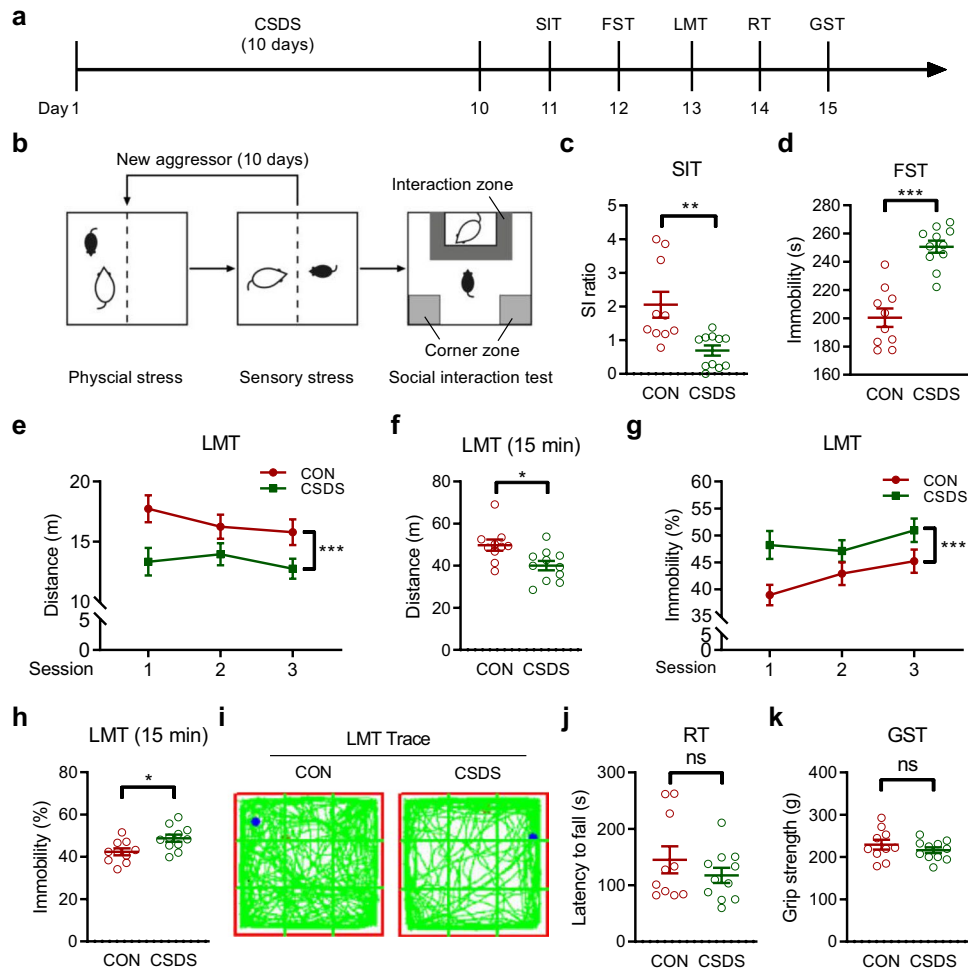


**Fig. 1** Spontaneous locomotor activity, but not passive motor activity, was reduced in chronic social defeat stress (CSDS) mice. **a** Timeline of CSDS treatments and behavioral tests. Social interaction test, SIT; forced swim test, FST; locomotion test, LMT; rotarod test, RT; grip strength test, GST. **b** Schematic of social defeat procedures and SIT. **c** Social interaction (SI) ratio [(interaction time, target present) / (interaction time, target absent)] was measured in CSDS individuals and control (CON) mice (unpaired *t* test,  $t = 3.427$ ,  $P = 0.0028$ ). **d** CSDS induced a depression-like phenotype in mice as assessed by immobility time in the forced swim test (FST, unpaired *t* test,  $t = 6.568$ ,  $P < 0.0001$ ). **e** Time course (three sessions and 5 min for each session) of spontaneous exploration in LMT with control and stressed mice (two-way ANOVA, row factor  $F_{(2,57)} = 0.804$ ,  $P = 0.4525$ ; column factor  $F_{(1,57)} = 15.28$ ,  $P = 0.0002$ ; interaction  $F_{(2,57)} = 0.557$ ,  $P = 0.5759$ ). **f** Total distance travelled for the 15-min locomotion test

in stressed and control mice (unpaired *t* test,  $t = 2.836$ ,  $P = 0.0106$ ). **g** The percentage of immobility time travelled during the three sessions with 5 min for each session (two-way ANOVA, row factor  $F_{(2,57)} = 2.214$ ,  $P = 0.1185$ ; column factor  $F_{(1,57)} = 12.92$ ,  $P = 0.0007$ ; interaction  $F_{(2,57)} = 0.714$ ,  $P = 0.494$ ). **h** The percentage of immobility time travelled in the 15-min locomotion test between stressed mice and control animals (unpaired *t* test,  $t = 2.713$ ,  $P = 0.0138$ ). **i** Representative trace of spontaneous locomotor activity for 15 min in control and stressed mice. **j** The latency to fall in RT was measured (unpaired *t* test,  $t = 1.037$ ,  $P = 0.3126$ ). **k** GST was performed by a dynamometer (unpaired *t* test,  $t = 1.008$ ,  $P = 0.3263$ ). The number of animals in control and CSDS group was 10 and 11, respectively. Data are depicted by the means  $\pm$  s.e.m. with \* $P < 0.05$ , \*\* $P < 0.01$ , and \*\*\* $P < 0.001$ . ns, no significant difference

mouse placed in the plexiglass cage. The times spent in the interaction zone surrounding the cage were measured by the Shanghai Xinruan video-tracking software. The social interaction ratio (SI ratio) was calculated as the time spent in the interaction zone (target) divided by the time spent in the interaction zone (no target).

### Forced Swim Test

Mice were individually placed into a cylindrical tank (30 cm height and 15 cm diameter) containing 20 cm of water (24 to 26 °C), in which the experiments could not touch the bottom of the tank. After 6 min, they were transferred to a drying environment. The water was changed after each test to avoid the influence of pheromone compounds left behind by the previous mice. The immobility time was measured with a video-tracking system (Shanghai Xinruan Information Technology Co. Ltd, Shanghai, China). Mice were considered immobile when floating and making only the necessary behaviors for keeping their nose above the water [16].

### Spontaneous Locomotor Activity Test

An automated video-tracking apparatus (Shanghai Xinruan Information Technology Co. Ltd) was used to assess spontaneous locomotion as previously described [17]. Mice were placed into the testing room 60 min before initiation of locomotion testing for acclimation to the testing surroundings. Animals were individually placed in the center of a gray frosting Plexiglas cage (50 cm × 50 cm × 50 cm), and spontaneous locomotor activity was measured in three sessions for 15 min total and 5 min for each session.

### Rotarod Test

Firstly, mice were habituated to the rotarod for 30 min and then became familiar with the rotarod by being subjected to one trial. After acclimation to the testing room for 60 min, mice were placed on the Rota-Rod (Ugo Basile, Gemonio VA, Italy), which was rotated at an accelerated speed from 4 to 40 rpm over a maximum of 5 min [18]. Each mouse was given four trials. Each trial ended when a mouse fell off or reached 300 s. The average latency to fall off the Rota-Rod was calculated.

### Grip Strength Test

The grip strength test was used to measure the maximal muscle strength of forelimbs in mice [19]. Mice were allowed to hold a metal grid with their forelimbs, lifted mice by the tail so that the hind limbs were not in contact with the grid, and gently pulled back until they could no longer grasp the grid. A grip strength meter (Shandong Academy of Medical

Sciences, China) was connected to a sensor to record the strength (g). Four trials were carried out in succession to measure forelimb strength. The mean of at least four successful trials was calculated for each animal.

### Stereotaxic Virus Injection

Adult male mice were 8–12 weeks old at the time of surgery. Mice were anesthetized with an intraperitoneal injection of chloral hydrate (350 mg/kg) and xylazine (10 mg/kg) and then placed in a stereotaxic apparatus (68,030, RWD, China). The small holes were drilled into the skull over the target areas. The viruses were stereotaxically injected at 10–30  $\mu$ l/min into the targeting areas using a micro-syringe pump (Stoelting, USA) with a pulled glass needle (WPI, USA). It was mounted directly on the stereotaxic frame. After each injection, the needle was kept in place for 10 min before its withdrawal to allow proper diffusion of the virus. Mice recovered on a heating pad until they waked up. All experiments involving viral injections were conducted at least 21 days after a surgical procedure to allow for sufficient expression [20]. Coordinates used were as follows (relative to Bregma, midline, or Bregma surface): VTA: AP (anterior/posterior) – 3.20 mm, ML (medial/lateral)  $\pm$  0.5 mm, DV (dorsal/ventral) – 4.6 mm; SNr: AP – 3.20 mm, ML 1.2 mm, DV – 4.7 mm.

### Immunohistochemistry and Imaging

Mice were deeply anesthetized and transcardially perfused with 4% paraformaldehyde (PFA) in 0.1 M phosphate-buffered saline (PBS). Brains were post-fixed for 1 day and placed in 30% sucrose in PBS for 1–2 days. After embedding, frozen sections were performed at 20 or 40  $\mu$ m thickness on a cryostat by microtome (CM1860, Leica, German). For immunohistochemistry, 20  $\mu$ m coronal sections were pretreated in 0.3% Triton X-100 for 5 min at room temperature, and then blocked in 10% goat serum albumin in PBS for 1 h at room temperature, and they were then incubated for overnight at 4 °C with primary antibody solution in PBS. On the following day, tissue was rinsed in PBS, reacted with secondary antibody for 1 h at room temperature, and rinsed again. The primary antibody used in the research was rabbit anti-tyrosine hydroxylase (TH, 1:200; Proteintech). The secondary antibodies used were Alexa Fluor 488 goat anti-rabbit (1:400, Jackson ImmunoResearch). For tracing analyses, 40  $\mu$ m coronal sections were just washed with PBS. The fluorescent images were obtained on an epifluorescence microscope (Olympus, Japan), an automatic scanning fluorescence microscope (Olympus, SV120), and a confocal microscopy (Zeiss, LSM800). The VTA sections were sampled continuously at least three slices at Bregma – 3.28 mm for each



mouse. Then, the average percentage of mCherry<sup>+</sup>TH<sup>+</sup>/TH<sup>+</sup> in each mouse was selected for statistical analysis.

### Chemogenetic Manipulation

To test the necessity of VTA-DA neuron activity for the development of CSDS-induced abnormal activity, 300 nl of a 1:1 volume mixture of AAV9-TH-Cre and AAV9-DIO-hM3Dq (Gq)-mCherry was injected bilaterally into the VTA of WT animals [21]. Mice were allowed 3 weeks to recover for sufficient expression. Clozapine-N-oxide (CNO, Sigma, 3 mg/kg) and saline were intraperitoneally delivered 1 h before the beginning of the behavioral testing. To activate VTA-DA neurons that project to the SNr, 200 nl of AAV2-retro-DIO-hM3Dq-mCherry was delivered bilaterally into the SNr, and 100 nl of AAV9-TH-Cre was injected into the VTA of WT mice. Three weeks later, animals were subjected to behavioral tests at 1 h after CNO injection as previously described [22].

### Multi-electrode Assay Recordings

Mice were anesthetized with chloral hydrate (350 mg/kg) and xylazine (10 mg/kg) and killed by decapitation. The brain was removed from the skull and the coronal midbrain slices (250 μm) containing VTA were cut by a vibratome (Leica, VT1000S) with high-sucrose ice-cold artificial cerebrospinal fluid (ACSF) containing (in mM): 230 sucrose, 10 glucose, 25 NaHCO<sub>3</sub>, 2.5 KCl, 1.2 NaH<sub>2</sub>PO<sub>4</sub>, 0.5 CaCl<sub>2</sub>, 7 MgCl<sub>2</sub>, and oxygenated with 95% O<sub>2</sub> / 5% CO<sub>2</sub>. Then, the slices were incubated for recovery at 32–34 °C for 60 min in ACSF containing the following (in mM): 120 NaCl, 10 glucose, 25 NaHCO<sub>3</sub>, 2.5 KCl, 1.2 NaH<sub>2</sub>PO<sub>4</sub>, 2.5 CaCl<sub>2</sub>, 2.3 MgCl<sub>2</sub>. After recovery, one slice was removed and placed in the recording chamber and perfused continuously with ACSF at 30 °C. Multi-electrode array (MEA) recordings were used to detect the firing rate of multiple neurons, using the MED64 System (Alpha MED Sciences, Osaka, Japan). Coronal midbrain slices from injected mice were placed over an 8 × 8 microelectrodes array, each 50 × 50 μm in size, with an interpolar distance of 150 μm (Alpha MED 150 Sciences Inc., Osaka, Japan). During recording, the slice was perfused continuously with oxygenated-ACSF at 30 °C. The first recording was performed as a baseline and the second was done 5 min after perfusion of oxygenated-ACSF containing CNO (10 μM). For recording, the amplification factor was set as 1200 × and the sampling frequency as 20 kHz. Then, the recorded signals were filtered (0.1 ~ 10 kHz) using MOBIUS software (Alpha MED Sciences, Osaka, Japan). Meanwhile, the threshold of peak detection was set as the signal amplitude exceeds ± 3.2-fold change of the standard deviations of the noise.

### Whole-Brain Quantitative Mapping

On day 1, 300 nl of a 1:1 volume mixture of AAV9-TH-Cre and AAV9-DIO-ChR2-EYFP was injected into the VTA of 8-week-old wildtype (WT) mice. On day 21, the mice were subjected to CSDS for consecutive 10 days. On day 31, mice were perfused and brain tissue was processed and sectioned as described in the histology and imaging section. For VTA output quantification, images were taken from 3 consecutive sections in each of the brain regions on an automated slide scanner with a 10 × objective and an argon laser at 488 nm (Carl Zeiss LSM-780 laser scanning confocal microscope, Zeiss Microsystems, Jena, Germany). Output signals (EYFP-positive) were assigned to specific brain regions based on the Allen Brain Atlas (<http://mouse.brain-map.org/static/atlas>). The result of representative coronal images for VTA-DA neurons projecting to regions was shown as a progression from anterior to posterior (AP). The pixel densities of these images were measured by Image J (Fiji) and averaged (3 images per brain region) to determine the fraction of axons resulting from VTA-DA neurons in each brain area. Because each brain differed in EYFP signals of brain region injected, we normalized EYFP signals in each brain region by EYFP signals of brain region injected in the same brain [23].

### Optogenetic Manipulations

To optical stimulate VTA-SNr pathway, 200 nl of AAV2-retro-DIO-ChR2-mCherry or AAV2-retro-DIO-mCherry virus was bilaterally injected into the SNr, and 100 nl of AAV9-TH-Cre was bilaterally injected into the VTA of WT mice. To optogenetic inhibit the VTA-SNr circuit, the AAV2-retro-DIO-eNpHR3.0-mCherry virus was employed. After 3 weeks, the mice were implanted bilaterally with custom-made optical fibers (200 μm core, 5 mm length) at a 7° angle into the VTA (AP – 3.2 mm; LM ± 1.05 mm; DV – 4.4 mm) and fixed using dental cement. Mice were allowed to recover for 7 days before starting behavioral testing. Optical fibers were connected using a laser generator (NEWDOON, Hangzhou, China) was used to generate blue light pulses (473 nm) or yellow light pulses (594 nm). Mice were given either 0.5 Hz, 15 ms (tonic firing) or 20 Hz, 40 ms (phasic firing) light stimulations and received 3 min stimulation during the locomotion test. In both tonic and phasic light stimulation protocols, VTA-DA neurons were exposed to 5 spikes over each 10 s [9]. Meanwhile, the mice within yellow light group were administrated 5 min with continuous stimulation at 10mW (laser power at the tip of the optic fiber) in behavior test.

## Data Analyses and Statistics

Statistical analyses were calculated using GraphPad Prism 7 software (GraphPad Software, Inc., San Diego, CA). Sample size was determined based on the numbers reported in the related research field. If the sample size is lower than 5, a test for normality (Shapiro–Wilk test) was conducted before parametric test. Statistical significance was determined by unpaired Student's *t*-tests, paired *t*-test, one-way analysis of variance (abbreviated one-way ANOVA), and two-way ANOVA according to the type of data sets. All data were presented as means  $\pm$  s.e.m. For all figures, ns represents *P*-value no less than 0.05; \**P* < 0.05; \*\**P* < 0.01 and \*\*\**P* < 0.001.

## Results

### Chronic Social Defeat Stress Greatly Affects the Spontaneous Locomotor Activity of Mice but Showed Little Influence on the Forced Locomotor Ability

To examine the spontaneous locomotor activity, mice exposed to CSDS were subjected to the locomotor activity test (LMT), along with several other behavioral tests relevant to forced motor ability (Fig. 1a). Mice were subjected to a standardized 10-day social defeat protocol and tested for avoidance behavior by the social interaction test (SIT) (Fig. 1b), as described previously [7]. After CSDS, defeated mice showed robust social aversion in the presence of a CD1 aggressor [24], whereas the social interaction score of control mice was significantly higher than CSDS mice (Fig. 1c). In the forced swim test (FST), CSDS mice had substantially longer immobile time than did control mice (Fig. 1d). Next, we tested the spontaneous locomotion performance using LMT in mice exhibiting depression-like behaviors. Stressed mice displayed significantly decreased distances travelled compared with unstressed mice (Fig. 1e and f); the immobility of CSDS mice was also higher than the control (Fig. 1g and h). Representative examples of the moving trace (15 min) between control and CSDS mice also exhibited significant differences (Fig. 1i). The ratio of distance travelled and time spent between the central and the peripheral area was no significantly altered after CSDS treatment (Supplementary Fig. 1a and b). Finally, we assessed whether the decline of the locomotor ability in CSDS mice was due to the physical injuries from CD1 aggressor mice. The mice exposed to the 10-day defeat stress were subjected to the rotarod test (RT) and grip strength test (GST). No significant differences between CSDS and control mice were observed (Fig. 1j and k). Collectively, our results demonstrated that CSDS triggered decreased locomotor activity.

### Targeted Activation of VTA-DA Neurons Rescued the CSDS-Induced Impairment of Locomotor Activity

VTA-DA neurons are critical for the development of CSDS-induced depression-related behaviors [25]. We first examined the electrophysiological characterization of VTA-DA neurons by multi-channel in vivo recording after the CSDS exposure. The electrophysiological result showed that the firing rate of putative VTA-DA neurons was significantly decreased after CSDS treatment (Supplementary Fig. 2a–d). To determine whether VTA-DA neuron activity was necessary for CSDS-induced behavioral adaptations, we used a chemogenetic approach to activate VTA-DA neurons selectively. Additionally, we took advantage of a recombinant AAV reporter virus expressing Cre recombinase under the TH promotor [21], and a Cre-dependent adeno-associated virus-containing hM3Dq. A mixture of AAV-TH-Cre and AAV-DIO-hM3Dq-mCherry virus was bilaterally injected into the VTA (Fig. 2a and b) to activate VTA-DA neurons selectively. To validate the chemogenetic tools, the infection efficiency of hM3Dq in VTA-DA neurons of wild-type mice was verified from brain slices (Fig. 2c and d). Meanwhile, treating with CNO robustly increased the VTA-DA neurons firing in hM3Dq-expressing mice (Fig. 2e and f). After the recovery process of 3 weeks, mice were subjected to the CSDS procedure, and locomotor activity was measured (Fig. 2g). Then, mice were injected saline or CNO (3 mg/kg, i.p.) 1 h before the behavioral tests. The CNO group had more locomotor activity compared with the NS group (Fig. 2h–l), indicating that stimulation of VTA-DA neurons reverses CSDS-induced hypolocomotion. Meanwhile, the ratio of distance travelled and time spent between the central and the peripheral area was no significantly changed in CNO group (Supplementary Fig. 3a and b).

### Whole-Brain Quantitative Mapping for CSDS-Induced VTA-DA Neuronal Outputs

Although the modification of VTA-DA neuronal firing has been clarified previously in mouse model of depression-relevant neurobehavioral states [25], the direct projections from VTA-DA neurons in CSDS compared with healthy mice remained unknown. Thus, to determine the identities of the VTA-DA neuronal projections altered by CSDS, we combined a recombinant AAV reporter virus expressing Cre recombinase under the tyrosine hydroxylase (TH) promoter and a Cre-dependent adeno-associated virus encoding ChR2-EYFP. All mice were subjected to CSDS treatment after injection with a mixture of AAV-TH-Cre and AAV-DIO-ChR2-mCherry into the VTA (Fig. 3a–c). As expected, robust anterograde tracing from the left VTA-DA neurons was observed throughout the brain (Fig. 3d, Supplementary

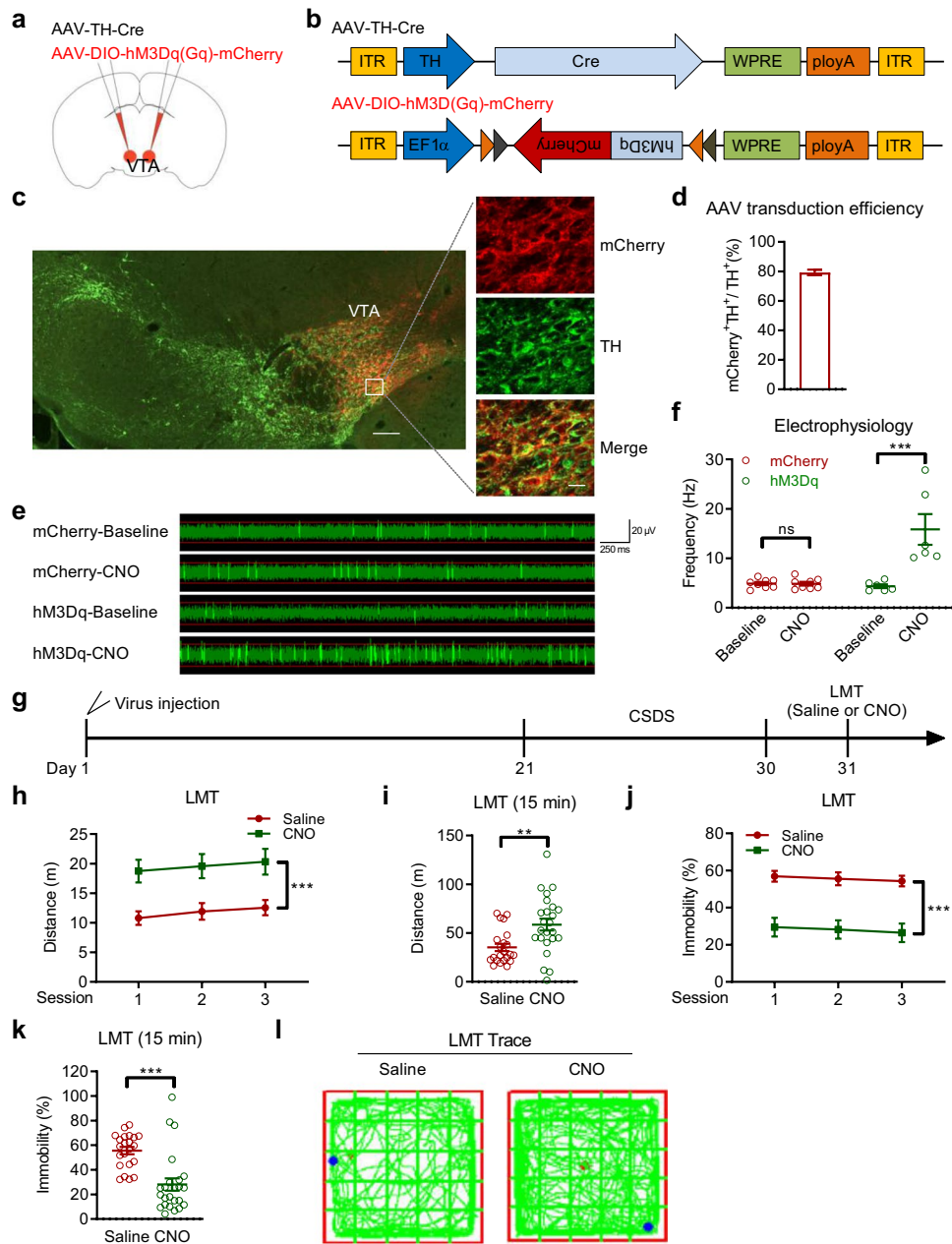


**Fig. 2** Chemogenetic activation of ventral tegmental area (VTA) dopamine neurons could reverse the chronic social defeat stress-induced impairment of locomotor activity. **a** A mixture of AAV-TH-Cre and AAV-DIO-hM3Dq-mCherry was injected into the VTA of WT mice. **b** Schematic map of AAV vector constructs. **c** Immunofluorescence image of AAV labeling (mCherry, red) in VTA dopamine neurons by the tyrosine hydroxylase (TH, green) antibody (scale bar, 125  $\mu$ m). Representative high-magnification images of immunofluorescence for mCherry and TH (scale bar, 25  $\mu$ m). **d** AAV transduction efficiency shows that mCherry and TH double-positive cells are  $79.28 \pm 1.87\%$  of total TH-positive neurons in the VTA ( $n=5$  mice). **e** Representative trace of spontaneous activity in the VTA region by the  $8 \times 8$  microelectrode array. **f** Scatter dot plot depicting the frequency of VTA cells in all groups. The number of mice was  $n=8$  for mCherry and  $n=6$  for hM3Dq group (paired  $t$ -test, mCherry/Baseline vs. mCherry/CNO,  $t=0.1768$ ,  $P=0.8647$ ; hM3Dq/Baseline vs. hM3Dq/CNO,  $t=3.843$ ,  $P=0.0121$ ). **g** Experimental timeline of

CSDS treatment and AAV injection. **h** The time-course distance travelled was detected by spontaneous locomotor activity in Saline and CNO mice during the three sessions with 5 min for each session (two-way ANOVA, row factor  $F_{(2,132)}=0.4605$ ,  $P=0.6320$ ; column factor  $F_{(1,132)}=29.8$ ,  $P<0.0001$ ; interaction  $F_{(2,132)}=0.0035$ ,  $P=0.9965$ ). **i** The total distance travelled in the 15-min locomotion test (unpaired  $t$  test,  $t=3.19$ ,  $P=0.0026$ ). **j** The percentage of immobility time travelled during the three sessions with 5 min for each session (Two-way ANOVA, row factor  $F_{(2,132)}=0.2231$ ,  $P=0.8003$ ; column factor  $F_{(1,132)}=62.91$ ,  $P<0.0001$ ; interaction  $F_{(2,132)}=0.0026$ ,  $P=0.9974$ ). **k** The immobility of the 15-min locomotion test (unpaired  $t$  test,  $t=4.642$ ,  $P<0.0001$ ). **l** Representative trace of the locomotion test for 15 min in Saline and CNO groups. The number of animals was 22 and 24 in the Saline and CNO groups, respectively. Data are displayed by the means  $\pm$  s.e.m. \* $P<0.05$ , \*\* $P<0.01$ , and \*\*\* $P<0.001$ . The ns showing no significant difference

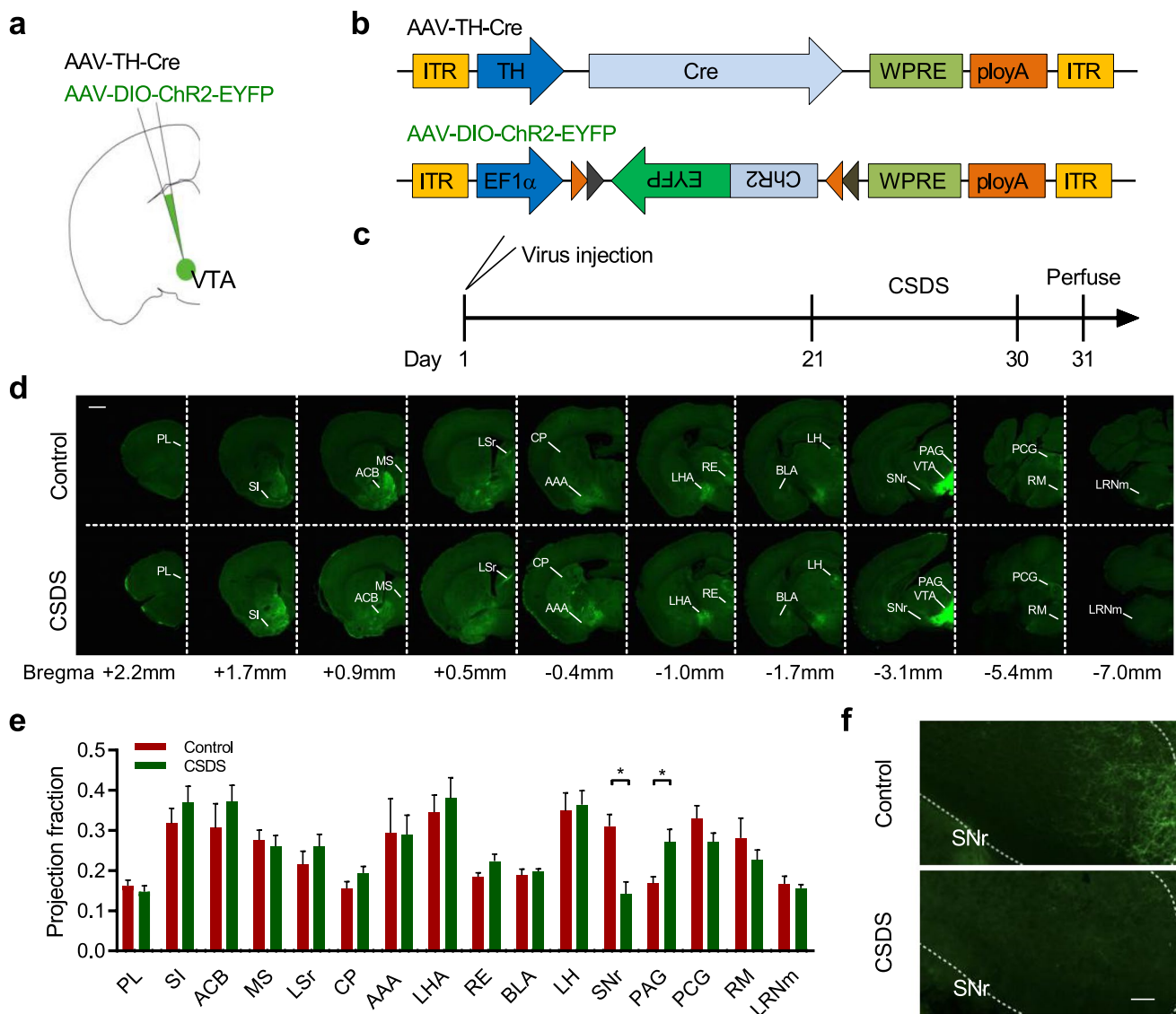


**Fig. 3** Whole-brain mapping of the outputs of ventral tegmental area (VTA) dopamine neurons in chronic social defeat stress mice. **a** A mixture of AAV-TH-Cre and AAV-DIO-ChR2-EYFP was unilaterally injected into the VTA of WT mice. **b** Schematic representation of viral vectors. **c** Experimental timeline of CSDS procedures and AAV injection. **d** Series of coronal sections from VTA-DA neurons in control and stressed mice after injection of the virus mixture (scale bar, 500  $\mu$ m). PL, prelimbic area; SI, substantia innominata; ACB, nucleus accumbens; MS, medial septal nucleus; LSr, lateral septal nucleus rostral part; CP, caudoputamen; AAA, anterior amygdalar area; LHA, lateral hypothalamic area; RE, nucleus of reuniens; BLA, basolateral amygdalar nucleus; LH, lateral habenula; SNr, substantia

nigra pars reticulata; VTA, ventral tegmental area; PAG, periaqueductal gray; PCG, pontine central gray; RM, nucleus raphe magnus; LRNm, lateral reticular nucleus, magnocellular part. **e** Average fraction of VTA-DA axons in 16 brain regions. Projection fractions were normalized by the fluorescence density of the injection site. (Control,  $n=3$ ; CSDS,  $n=3$ ; unpaired  $t$ -test; SNr,  $t=3.991$ ,  $P=0.0163$ ; PAG,  $t=2.854$ ,  $P=0.0462$ .) **f** Representative image of the substantia nigra pars reticulata (SNr) region in stressed and control animals (scale bar, 100  $\mu$ m). Data are represented by the means  $\pm$  s.e.m. \* $P<0.05$ , \*\* $P<0.01$ , and \*\*\* $P<0.001$ . The detailed statistical values were shown as Supplementary Table 1

**Fig. 4**. Strong projections were seen in the prelimbic area (PL), substantia innominata (SI), nucleus accumbens (ACB), medial septal nucleus (MS), lateral septal nucleus rostral part (LSr), caudoputamen (CP), anterior amygdalar area (AAA), lateral hypothalamic area (LHA), nucleus of reuniens (RE), basolateral amygdalar nucleus (BLA), lateral habenula (LH), SNr, periaqueductal gray (PAG), pontine

central gray (PCG), nucleus raphe magnus (RM), and lateral reticular nucleus magnocellular part (LRNm). Analysis of the labeled projections from VTA-DA neurons in 16 brain regions, comprised of long-range outputs, revealed significant differences of SNr and PAG between the control and CSDS groups (Fig. 3e, Supplementary Fig. 5). Moreover, representative images of EYFP-positive terminals in the



SNr are shown (Fig. 3f). Our results indicated that VTA-DA neurons projected to SNr, and the VTA-SNr outputs were significantly decreased in CSDS.

### Chemogenetic Activation of VTA-SNr Projections Reversed the CSDS-Induced Hypolocomotion

Given that the VTA-SNr dopaminergic projections were significantly reduced in CSDS, selective chemogenetic activation of this circuit may also restore the locomotor activity performance in CSDS mice. To specifically manipulate the neural circuit from the VTA-DA to SNr, we expressed hM3Dq in the VTA-SNr circuit by bilaterally injecting a recombinant AAV reporter virus expressing Cre recombinase driven by the TH promoter (AAV-TH-Cre) into the VTA, and a retrograde Cre-dependent adeno-associated virus encoding hM3Dq (AAV-retro-DIO-hM3Dq-mCherry) separately into the SNr (Fig. 4a and b). The infection efficiency of hM3Dq in VTA-DA neurons was confirmed by immunofluorescence staining (Fig. 4c and d). Furthermore, the VTA-DA neurons activity was validated by electrophysiology (Fig. 4e and f). According to the experimental timeline (Fig. 4g), infected mice were exposed to the 10-day social defeat stress protocol before starting the behavioral test. The results suggested that the CNO-mediated activation of VTA-SNr projections reversed the CSDS-induced hypolocomotion (Fig. 4h–l). And the ratio of distance travelled and time spent between the central and the peripheral area was not significantly changed in CNO group (Supplementary Fig. 6a and b).

### Selectively Phasic Optogenetic Stimulation of the VTA-SNr Circuit Generates Hyperlocomotion

To selectively activate the circuit of VTA-DA neurons to the SNr by optogenetic tools, mice were given stereotaxic injections of a recombinant AAV reporter virus expressing Cre recombinase controlled by the TH promoter (AAV-TH-Cre), and a retrograde adeno-associated virus with Cre-dependent constructs encoding ChR2 (AAV-retro-DIO-ChR2-mCherry), into the VTA and SNr, respectively. Optic fibers were implanted in the VTA before behavioral testing (Fig. 5a and b). The experimental timeline is shown in Fig. 5c. To assess the functional consequence of increased neuronal firing in VTA-SNr projections, the behavioral effects of optogenetic-induced phasic firing (20 Hz, 40 ms), with 5 spikes for each 10 s, in ChR2-expressing VTA-DA neurons were evaluated during locomotion testing (Fig. 5d). Mice that received phasic stimulation (ChR2 group) expressed a robust increase in locomotion, indicated by significant increases in travel distance and decreased immobility compared with phasic-stimulated mCherry control mice (Fig. 5e–i). And the ratio of distance travelled and time

spent between the central and the peripheral area was no significantly altered in ChR2 group (Supplementary Fig. 7a and b). However, mice stimulated with tonic firing (0.5 Hz, 15 ms) (Fig. 6a) showed no significant differences in travel distance or immobility between ChR2 and mCherry groups (Fig. 6b–g) during behavioral testing. The ratio of distance travelled and time spent between the central and the peripheral area was not significantly changed in ChR2 mice (Supplementary Fig. 8a and b). These data confirmed the functional importance of VTA-SNr projections through enhanced phasic firing, but not tonic firing, which was involved in the hyperactivity.

## Discussion

Although there are some drugs, like fluoxetine, that could be significantly relieving or treating MDD, the pathophysiological mechanism underlying depression is still a major challenge in psychiatric research. In this study, we combined behavioral assays, viral tracing, chemogenetics, optogenetics, and immunofluorescence to elucidate how the VTA-SNr dopaminergic projection mediates the hypolocomotion behaviors in CSDS mice model. Firstly, we found CSDS could directly induce a decline in locomotor activity performance, but not motor ability. Secondly, using chemogenetic technology, we modulated VTA-DA neuron activity and found that VTA-DA neuron activation ameliorated CSDS-induced hypolocomotion. Thirdly, the alteration of all the brain regions, which receives VTA-DA neuronal projections, was identified and quantitated in depressive mice. Lastly, the dopaminergic projections from VTA to SNr were functionally validated in CSDS-induced hypolocomotion performance.

An initial objective of this study was to identify whether the locomotor activity changed in CSDS individuals. Our results showed that the CSDS triggered decreased locomotor activity and increased immobility. This finding observed in this study mirrors those of the previous study that have examined the behavior outcomes of social defeat stress in Lewis rats [6]. However, the locomotor activity displayed no significant alterations in the chronic mild stress animal model [25]. The reason for the inconsistency of locomotion performance between CSDS and chronic mild stress model is not clear but it may have something to do with the different protocols for establishing the animal model of depression-relevant neurobehavioral states. A unique aspect of the CSDS mouse model that distinguishes from other environmental stressors is its ability to continuously activate the pituitary-adrenal axis over 10 consecutive days of repeated social confrontations [26]. It is also worth noting that the potential pitfalls of utilizing the CSDS model, as well as of any animal model based on social interaction, include the

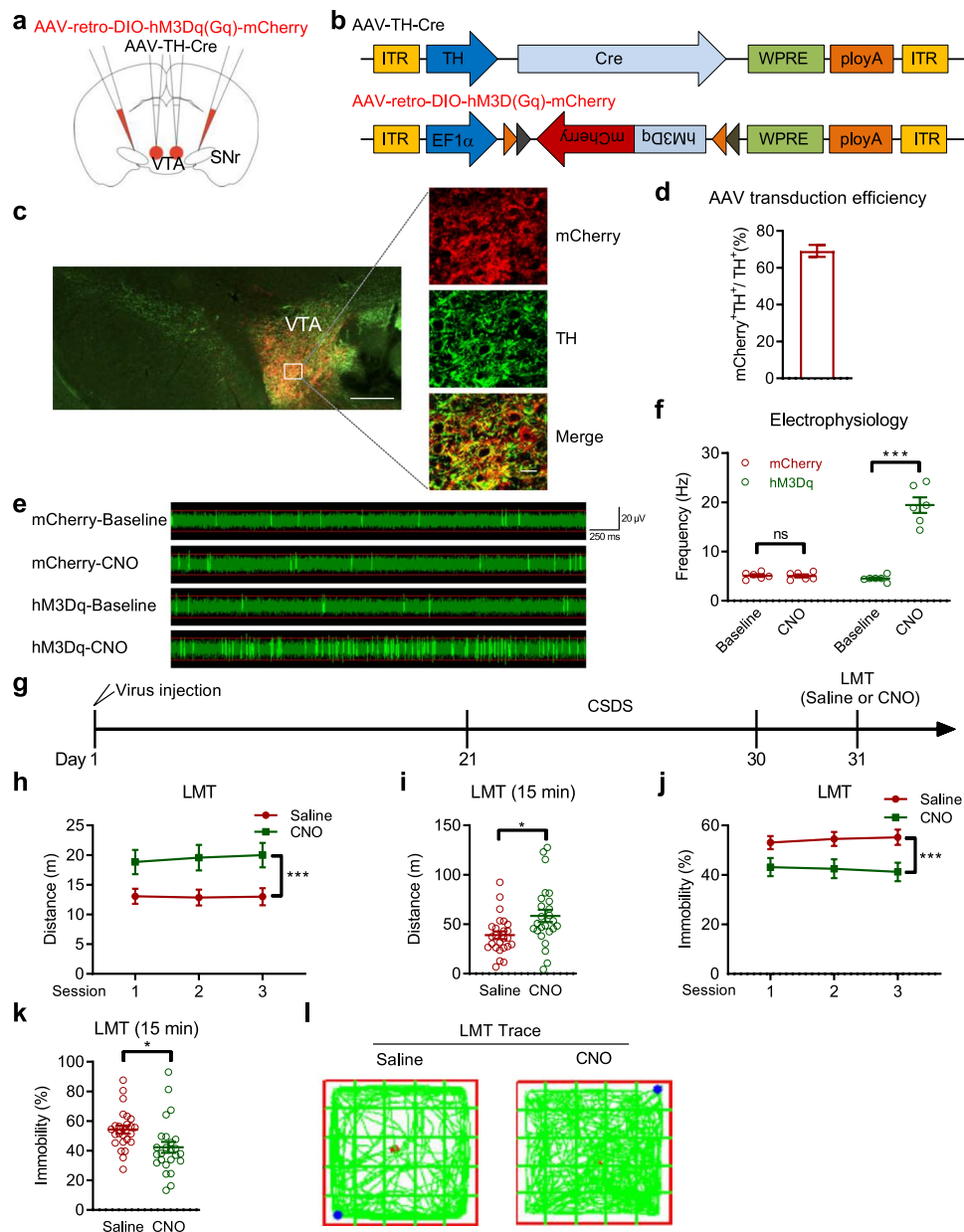


**Fig. 4** Chemogenetic activation of the ventral tegmental area to substantia nigra pars reticulata (VTA-SNr) projections could rescue the chronic social defeat stress (CSDS)-induced hypocomotion. **a** AAV-TH-Cre and AAV-retro-DIO-hM3Dq(Gq)-mCherry was bilaterally injected respectively into the VTA and SNr of WT mice. **b** Schematic representation of AAV vectors. **c** Representative image of TH-positive neurons labeled mCherry in VTA (scale bar=250  $\mu$ m). High-magnification images of immunofluorescence for mCherry and TH (scale bar, 25  $\mu$ m). **d** AAV transduction efficiency shows that mCherry and TH double-positive cells are  $69.11 \pm 3.26\%$  of total TH positive neurons in the VTA area ( $n=9$  mice). **e** Representative trace of spontaneous activity in the VTA region by microelectrode array. **f** Scatter dot plot showing the frequency of VTA cells. The number of mice was  $n=8$  for mCherry and  $n=6$  for hM3Dq group (paired  $t$ -test, mCherry/Baseline vs. mCherry/CNO,  $t=0.3496$ ,  $P=0.7409$ ; hM3Dq/Baseline vs. hM3Dq/CNO,  $t=9.015$ ,  $P=0.0003$ ). **g** Timeline of AAV injection and behavior tests. **h** The distance travelled of

time points (three sessions with 5 min for each session) was measured by the locomotion test in Saline and CNO groups (two-way ANOVA, row factor  $F_{(2,144)}=0.0492$ ,  $P=0.9520$ ; column factor  $F_{(1,144)}=20.51$ ,  $P<0.0001$ ; interaction  $F_{(2,144)}=0.0669$ ,  $P=0.9353$ ). **i** The total distance travelled of the 15-min locomotion test in Saline and CNO mice (unpaired  $t$  test,  $t=2.665$ ,  $P=0.0104$ ). **j** The immobility of time points (three sessions with 5 min for each session) in locomotion test (two-way ANOVA, row factor  $F_{(2,144)}=0.0085$ ,  $P=0.9915$ ; column factor  $F_{(1,144)}=19.36$ ,  $P<0.0001$ ; interaction  $F_{(2,144)}=0.1863$ ,  $P=0.8302$ ). **k** The immobility of the locomotion test for a 15-min period was recorded in Saline and CNO groups (unpaired  $t$  test,  $t=2.633$ ,  $P=0.0114$ ). **l** Representative trace of the locomotion test for 15 min in Saline and CNO mice. The number of mice was  $n=25$  for both Saline and CNO groups. Data are depicted by the mean  $\pm$  s.e.m. \* $P<0.05$ , \*\* $P<0.01$ , and \*\*\* $P<0.001$ . ns, no significant difference

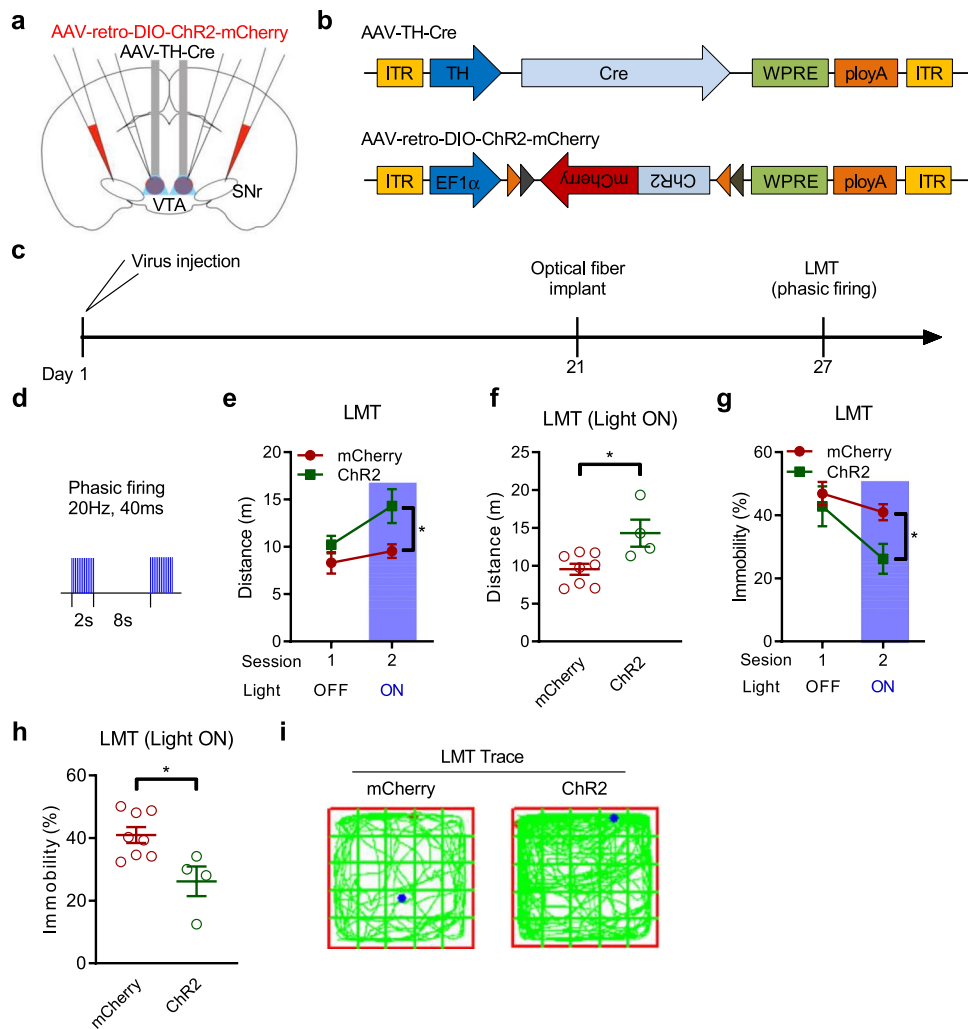


**Fig. 5** Optogenetic stimulation with phasic firing of the ventral tegmental area to substantia nigra pars reticulata (VTA-SNr) circuit induced hyperlocomotion in mice. **a** Diagram of virus injection and optical fiber implant in wildtype mice to activate the VTA-SNr circuit. **b** Schematic representation of AAV vectors. **c** Project timeline of virus injection and optical fiber implant. **d** Optogenetic stimulation protocols for mimicking phasic (20 Hz, 40 ms) with blue light (470 nm). **e** The distance travelled of the locomotion test was measured during the lights off and on (two sessions with 3 min for each session), with phasic optogenetic stimulation (two-way ANOVA, row factor  $F_{(1,20)}=5.023$ ,  $P=0.0365$ ; column factor  $F_{(1,20)}=7.967$ ,  $P=0.0105$ ; interaction  $F_{(1,20)}=1.434$ ,  $P=0.2451$ ). **f** The 3-min distance travelled of the locomotion test in mCherry and ChR2 groups

with lights on of phasic firing was conducted (unpaired  $t$  test,  $t=2.978$ ,  $P=0.0139$ ). **g** Percentage of time spent in the immobile state during lights off and on with phasic firing was displayed (two-way ANOVA, row factor  $F_{(1,20)}=7.251$ ,  $P=0.0140$ ; column factor  $F_{(1,20)}=5.057$ ,  $P=0.0360$ ; interaction  $F_{(1,20)}=1.644$ ,  $P=0.2145$ ). **h** Percentage of time spent in the immobile state after optical stimulation of phasic firing within a session for 3 min (unpaired  $t$  test,  $t=3.044$ ,  $P=0.0124$ ). **i** Characteristic trace from mCherry and ChR2 mice under the phasic firing stimulation condition. The number of mice was  $n=8$  for mCherry and  $n=4$  for ChR2 groups, with phasic firing. Data are showed by the means  $\pm$  s.e.m. \* $P<0.05$ , \*\* $P<0.01$ , and \*\*\* $P<0.001$ . The detailed information of statistical values was displayed as Supplementary Table 2

varying aggression levels of CD1 mice and the subjective classification of phenotypes (susceptibility or resilience) [7]. Certainly, the similarities and differences between CSDS and the chronic mild stress model were an important issue for future research.

VTA-DA neurons have been suggested that could directly project to various brain structures to involve in neuropsychiatric diseases [12]. Viral-genetic tracing tools as a new paradigm to tackle neural circuit research; however, few studies

have used this approach to analyze direct projections of the VTA-DA neurons in the CSDS-induced animal model of depression-relevant neurobehavioral states. This study identified SNr and PAG regions were the significantly changed targets receiving VTA-DA neuronal projections during the stress-induced depression. SNr is the major output nuclei of the basal ganglia circuit [27]. Meanwhile, the published study suggested that a higher strength SNr stimulation abolished the locomotion [28]. Reduced projections from the

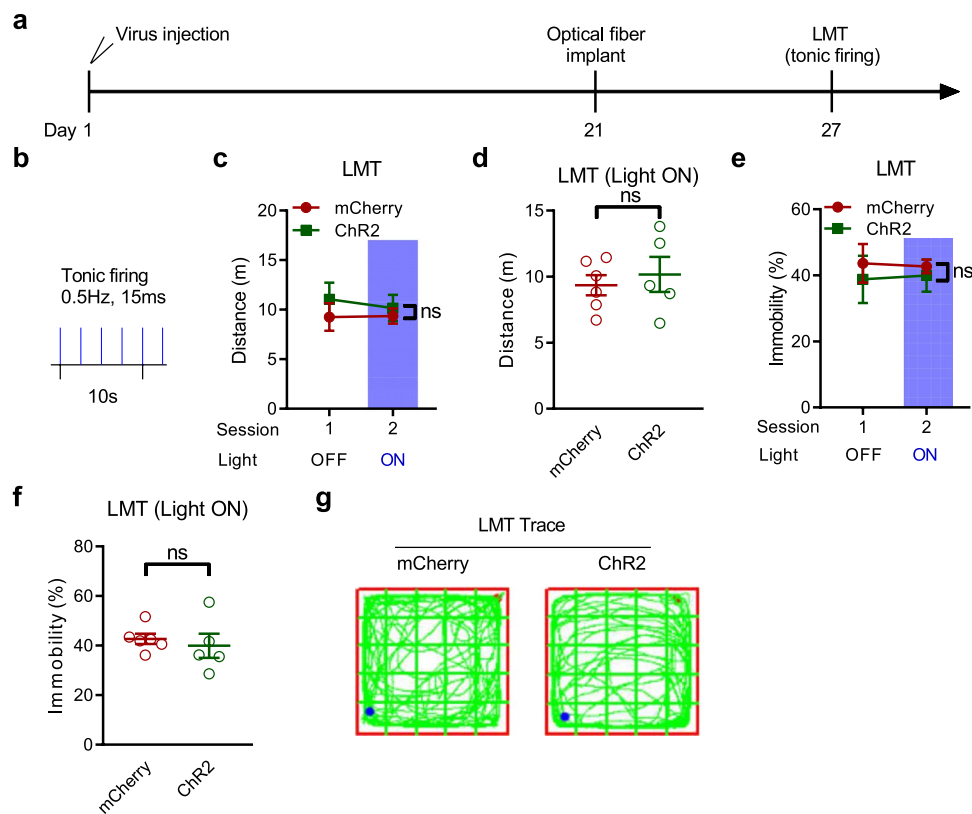


**Fig. 6** Optogenetic activation with tonic firing of the ventral tegmental area to substantia nigra pars reticulata (VTA-SNr) projections has no impact on locomotion. **a** Experimental timeline of treatments and behavior tests. **b** Optogenetic stimulation protocols for mimicking tonic (0.5 Hz, 15 ms) firing. **c** The distance travelled of the locomotion test was measured during the lights off and on (two sessions with 3 min for each session) with tonic optogenetic stimulation (two-way ANOVA, row factor  $F_{(1,18)}=0.0938$ ,  $P=0.7629$ ; column factor  $F_{(1,18)}=1.011$ ,  $P=0.3281$ ; interaction  $F_{(1,18)}=0.142$ ,  $P=0.7107$ ). **d** The distance travelled of the spontaneous locomotor activity with tonic firing during lights on within 3 min was recorded (unpaired  $t$

test,  $t=0.557$ ,  $P=0.5911$ ). **e** The immobility of the locomotion test was analyzed during lights off and on (two sessions with 3 min for each session) with tonic stimulation. (two-way ANOVA, row factor  $F_{(1,18)}=0.0004$ ,  $P=0.9838$ ; column factor  $F_{(1,18)}=0.5434$ ,  $P=0.4705$ ; interaction  $F_{(1,18)}=0.0396$ ,  $P=0.8445$ ). **f** Immobility of the locomotion test after tonic photo-stimulation with lights on for 3 min (unpaired  $t$  test,  $t=0.5636$ ,  $P=0.5868$ ). **g** Representative trace of mCherry and ChR2 mice after tonic optical stimulation with lights on. The mCherry and ChR2 groups with tonic firing were  $n=6$  and  $n=5$ , respectively. Data are represented by the means  $\pm$  s.e.m. ns; no significant difference

VTA-DA to the SNr appear to contribute to CSDS-induced hypolocomotion. This finding may support previous research into this crucial role, which links SNr and locomotion. Other dopaminergic projections from VTA-DA neurons to PAG were significantly increased after CSDS procedures treatment. A further study with more focus on the role of the VTA-PAG circuit in CSDS-induced hypolocomotion is therefore suggested.

Optogenetic-behavioral experiments revealed that phasic, but not tonic, stimulation of VTA-DA neurons could increase spontaneous locomotor activity. We also demonstrated that prolonged artificial activity of VTA-DA neuronal terminals in the SNr sufficiently reversed CSDS-induced locomotor decreases. The present findings seem to be consistent with other research which found dysfunction of dopamine neuron firing in the VTA is essential for the development of neuropsychiatric disorders such as depression [29]. The results

also suggested that the phasic firing pattern of VTA-DA neurons has a functional role in encoding locomotor activity performance. However, the precise firing of GABAergic neurons in the SNr controlled by VTA-DA projections requires further study. It is well known that the phasic firing of VTA-DA neurons encoding reward [30]. Meanwhile, the spontaneous locomotor activity test was based on free exploration and moving behavior. Hence, it could conceivably be hypothesized that such connections exist between reward and locomotion. However, more research on this topic needs to be undertaken before the association between depression-related hypolocomotion and reward deficits is more clearly understood.

In the current study, the generalizability of these findings is subject to certain limitations. Firstly, previously published studies have suggested that antidepressant bupropion, an inhibitor of dopamine reuptake, induces a dose-dependent



hyperlocomotion in adult mice [31, 32]. Thus, the dopaminergic projection of VTA-SNr maybe not only plays a role in MDD-specific hypolocomotion, but also participates in the physiological basis of spontaneous locomotion. Secondly, the present study was only selected male mice to study the neural basis of hypolocomotive behavior in CSDS model. Sex differences have been observed in MDD, and females show a roughly twofold greater risk as compared to males [33–35]. Therefore, the findings of this study cannot be extrapolated to female population. Thirdly, considering the validities of CSDS, not all exposed mice should develop depressive-like phenotype as not all chronically stress humans will experience MDD. It is important to bear in mind the possible bias of individual differences in response to CSDS treatment. Further studies, which take the variable of individual differences into account, will need to be undertaken. Fourthly, the spontaneous locomotor activity test was performed in an open field apparatus. It is well known the open field test is one of the most commonly used platforms to measure anxiety-like behaviors in animal models [36]. Several studies have revealed that repeated social defeat significantly induced anxiety-like behavior in CSDS mice [7, 37]. However, the ratio of distance travelled and time spent between the central and the peripheral area was no significantly changed in all spontaneous locomotor activity tests. The reason for this was that the tracking period of locomotor activity was much longer than anxiety-like behavior. The experimental mice may enter the central portions more readily due to habituation to the central area of the open field maze in the later period. Moreover, this study focuses on the VTA-SNr pathway in CSDS-induced hypolocomotion behavior. Undoubtedly, the CSDS-related anxiety-like behavior was also an important and interesting question. Further work needs to be done to establish how the VTA dopamine neurons regulate CSDS-related anxiety-like behavior.

In summary, we describe a neural circuit from VTA-DA neurons to SNr that maybe underlies the locomotor activity in hypolocomotive behavior observed in CSDS.

**Supplementary Information** The online version contains supplementary material available at <https://doi.org/10.1007/s12035-021-02522-7>.

**Acknowledgements** The authors wish to acknowledge Dr. Xutao Zhu, Dr. Sen Jin (Center for Brain Science, Innovation Academy for Precision Measurement Science and Technology, Chinese Academy of Sciences, Wuhan, 430071 China), and Dr. Manfei Deng (Department of Pathophysiology, School of Basic Medicine, Tongji Medical College, Huazhong University of Science and Technology, Wuhan, Hubei Province, 430030, P. R. China) for their technical assistance with this project.

**Author Contribution** F.H.: investigation, methodology, data curation, formal analysis, writing—original draft, visualization. P.Z.: conceptualization, methodology, data curation, formal analysis, writing—review

and editing, visualization, project administration, funding acquisition. Q.Z.: investigation, methodology, formal analysis, validation, visualization. G.J.Q.: validation, data curation, formal analysis, visualization. H.W.C.: investigation, formal analysis, validation, data curation. T.X.L.: investigation, validation, data curation. M.L.L.: investigation, validation, data curation. J.Z.L.: investigation, formal analysis. J.E.L.: investigation, formal analysis. J.M.: conceptualization, resources, supervision. B.T.: conceptualization, methodology, resources, writing—review and editing, visualization, supervision, project administration, funding acquisition.

**Funding** This work was supported financially by grants from National Natural Science Foundation of China (Nos. 31871073, 31571044 to B.T., and No. 31600821 to P.Z.), Program for New Century Excellent Talents in University (No. NCET-10-0415 to B.T.), and the Fundamental Research Funds for the Central Universities (HUST: 2019kfyXJJS081 to P.Z.).

**Data Availability** Data will be made available on reasonable request.

All animal handling and experiments were performed in accordance with NIH guidelines and reviewed by the Ethics Committees of Huazhong University of Science and Technology (HUST).

## Declarations

**Consent to Participate** Not applicable.

**Consent to Publish** Not applicable.

**Conflict of Interest** The authors declare no competing interests.

## References

1. Yoon G, Petrakis IL, Krystal JH (2019) Association of combined naltrexone and ketamine with depressive symptoms in a case series of patients with depression and alcohol use disorder. *JAMA Psychiat* 76(3):337–338. <https://doi.org/10.1001/jamapsychiatry.2018.3990>
2. Knowland D, Lilascharoen V, Pacia CP, Shin S, Wang EH, Lim BK (2017) Distinct ventral pallidum neural populations mediate separate symptoms of depression. *Cell* 170(2):284–2297 e218. <https://doi.org/10.1016/j.cell.2017.06.015>
3. Nestler EJ, Hyman SE (2010) Animal models of neuropsychiatric disorders. *Nat Neurosci* 13(10):1161–1169. <https://doi.org/10.1038/nn.2647>
4. Kalueff AV, Fox MA, Gallagher PS, Murphy DL (2007) Hypolocomotion, anxiety and serotonin syndrome-like behavior contribute to the complex phenotype of serotonin transporter knockout mice. *Genes Brain Behav* 6(4):389–400. <https://doi.org/10.1111/j.1601-183X.2006.00270.x>
5. Mogil JS, Graham AC, Ritchie J, Hughes SF, Austin JS, Schorscher-Petcu A, Langford DJ, Bennett GJ (2010) Hypolocomotion, asymmetrically directed behaviors (licking, lifting, flinching, and shaking) and dynamic weight bearing (gait) changes are not measures of neuropathic pain in mice. *Mol Pain* 6:34. <https://doi.org/10.1186/1744-8069-6-34>
6. Berton O, Aguerre S, Sarrieau A, Mormede P, Chaouloff F (1998) Differential effects of social stress on central serotonergic activity and emotional reactivity in Lewis and spontaneously hypertensive rats. *Neuroscience* 82(1):147–159. [https://doi.org/10.1016/s0306-4522\(97\)00282-0](https://doi.org/10.1016/s0306-4522(97)00282-0)

7. Golden SA, Covington HE 3rd, Berton O, Russo SJ (2011) A standardized protocol for repeated social defeat stress in mice. *Nat Protoc* 6(8):1183–1191. <https://doi.org/10.1038/nprot.2011.361>
8. Douma EH, de Kloet ER (2020) Stress-induced plasticity and functioning of ventral tegmental dopamine neurons. *Neurosci Biobehav Rev* 108:48–77. <https://doi.org/10.1016/j.neubiorev.2019.10.015>
9. Chaudhury D, Walsh JJ, Friedman AK, Juarez B, Ku SM, Koo JW, Ferguson D, Tsai HC et al (2013) Rapid regulation of depression-related behaviours by control of midbrain dopamine neurons. *Nature* 493(7433):532–536. <https://doi.org/10.1038/nature11713>
10. Matsumoto M, Hikosaka O (2009) Two types of dopamine neuron distinctly convey positive and negative motivational signals. *Nature* 459(7248):837–841. <https://doi.org/10.1038/nature08028>
11. Howe MW, Dombeck DA (2016) Rapid signalling in distinct dopaminergic axons during locomotion and reward. *Nature* 535(7613):505–510. <https://doi.org/10.1038/nature18942>
12. Morales M, Margolis EB (2017) Ventral tegmental area: cellular heterogeneity, connectivity and behaviour. *Nat Rev Neurosci* 18(2):73–85. <https://doi.org/10.1038/nrn.2016.165>
13. Grace AA, Floresco SB, Goto Y, Lodge DJ (2007) Regulation of firing of dopaminergic neurons and control of goal-directed behaviors. *Trends Neurosci* 30(5):220–227. <https://doi.org/10.1016/j.tins.2007.03.003>
14. Mohebi A, Pettibone JR, Hamid AA, Wong JT, Vinson LT, Patriarchi T, Tian L, Kennedy RT et al (2019) Dissociable dopamine dynamics for learning and motivation. *Nature* 570(7759):65–70. <https://doi.org/10.1038/s41586-019-1235-y>
15. Beier KT, Steinberg EE, DeLoach KE, Xie S, Miyamichi K, Schwarz L, Gao XJ, Kremer EJ, Malenka RC, Luo L (2015) Circuit architecture of VTA dopamine neurons revealed by systematic input-output mapping. *Cell* 162(3):622–634. <https://doi.org/10.1016/j.cell.2015.07.015>
16. Can A, Dao DT, Arad M, Terrillion CE, Piantadosi SC, Gould TD (2012) The mouse forced swim test. *J Vis Exp* 59:e3638. <https://doi.org/10.3791/3638>
17. Mei Y, Monteiro P, Zhou Y, Kim JA, Gao X, Fu Z, Feng G (2016) Adult restoration of Shank3 expression rescues selective autistic-like phenotypes. *Nature* 530(7591):481–484. <https://doi.org/10.1038/nature16971>
18. Orr AG, Hsiao EC, Wang MM, Ho K, Kim DH, Wang X, Guo W, Kang J et al (2015) Astrocytic adenosine receptor A2A and Gs-coupled signaling regulate memory. *Nat Neurosci* 18(3):423–434. <https://doi.org/10.1038/nn.3930>
19. Davies JE, Wang L, Garcia-Oroz L, Cook LJ, Vacher C, O'Donovan DG, Rubinsztein DC (2005) Doxycycline attenuates and delays toxicity of the oculopharyngeal muscular dystrophy mutation in transgenic mice. *Nat Med* 11(6):672–677. <https://doi.org/10.1038/nm1242>
20. Takeuchi T, Duzskiewicz AJ, Sonneborn A, Spooner PA, Yamasaki M, Watanabe M, Smith CC, Fernandez G et al (2016) Locus coeruleus and dopaminergic consolidation of everyday memory. *Nature* 537(7620):357–362. <https://doi.org/10.1038/nature19325>
21. Stauffer WR, Lak A, Yang A, Borel M, Paulsen O, Boyden ES, Schultz W (2016) Dopamine neuron-specific optogenetic stimulation in rhesus macaques. *Cell* 166(6):1564–1571 e1566. <https://doi.org/10.1016/j.cell.2016.08.024>
22. Beier KT, Kim CK, Hoerbel P, Hung LW, Heifets BD, DeLoach KE, Mosca TJ, Neuner S et al (2017) Rabies screen reveals GPe control of cocaine-triggered plasticity. *Nature* 549(7672):345–350. <https://doi.org/10.1038/nature23888>
23. Schwarz LA, Miyamichi K, Gao XJ, Beier KT, Weissbourd B, DeLoach KE, Ren J, Ibanes S et al (2015) Viral-genetic tracing of the input-output organization of a central noradrenaline circuit. *Nature* 524(7563):88–92. <https://doi.org/10.1038/nature14600>
24. Wu X, Liu BJ, Ji S, Wu JF, Xu CQ, Du YJ, You XF, Li B et al (2015) Social defeat stress promotes tumor growth and angiogenesis by upregulating vascular endothelial growth factor/extracellular signal-regulated kinase/matrix metalloproteinase signaling in a mouse model of lung carcinoma. *Mol Med Rep* 12(1):1405–1412. <https://doi.org/10.3892/mmr.2015.3559>
25. Tye KM, Mirzabekov JJ, Warden MR, Fencz EA, Tsai HC, Finkelstein J, Kim SY, Adhikari A et al (2013) Dopamine neurons modulate neural encoding and expression of depression-related behaviour. *Nature* 493(7433):537–541. <https://doi.org/10.1038/nature11740>
26. Macedo GC, Morita GM, Domingues LP, Favoretto CA, Suchecki D, Quadros IMH (2018) Consequences of continuous social defeat stress on anxiety- and depressive-like behaviors and ethanol reward in mice. *Horm Behav* 97:154–161. <https://doi.org/10.1016/j.yhbeh.2017.10.007>
27. Blandini F, Nappi G, Tassorelli C, Martignoni E (2000) Functional changes of the basal ganglia circuitry in Parkinson's disease. *Prog Neurobiol* 62(1):63–88
28. Takakusaki K, Habaguchi T, Ohtinata-Sugimoto J, Saitoh K, Sakamoto T (2003) Basal ganglia efferents to the brainstem centers controlling postural muscle tone and locomotion: a new concept for understanding motor disorders in basal ganglia dysfunction. *Neuroscience* 119(1):293–308. [https://doi.org/10.1016/s0306-4522\(03\)00095-2](https://doi.org/10.1016/s0306-4522(03)00095-2)
29. Nestler EJ, Carlezon WA Jr (2006) The mesolimbic dopamine reward circuit in depression. *Biol Psychiatry* 59(12):1151–1159. <https://doi.org/10.1016/j.biopsych.2005.09.018>
30. Tsai HC, Zhang F, Adamantidis A, Stuber GD, Bonci A, de Lecea L, Deisseroth K (2009) Phasic firing in dopaminergic neurons is sufficient for behavioral conditioning. *Science* 324(5930):1080–1084. <https://doi.org/10.1126/science.1168878>
31. Billes SK, Cowley MA (2008) Catecholamine reuptake inhibition causes weight loss by increasing locomotor activity and thermogenesis. *Neuropsychopharmacology* 33(6):1287–1297. <https://doi.org/10.1038/sj.npp.1301526>
32. Redolat R, Vidal J, Gomez MC, Carrasco MC (2005) Effects of acute bupropion administration on locomotor activity in adolescent and adult mice. *Behav Pharmacol* 16(1):59–62. <https://doi.org/10.1097/00008877-200502000-00007>
33. Sachs BD, Ni JR, Caron MG (2014) Sex differences in response to chronic mild stress and congenital serotonin deficiency. *Psychoneuroendocrinology* 40:123–129. <https://doi.org/10.1016/j.psyneuen.2013.11.008>
34. Duncan N, Zimmer-Gembeck MJ, Furman W (2019) Sexual harassment and appearance-based peer victimization: unique associations with emotional adjustment by gender and age. *J Adolesc* 75:12–21. <https://doi.org/10.1016/j.adolescence.2019.06.016>
35. LeGates TA, Kvarta MD, Thompson SM (2019) Sex differences in antidepressant efficacy. *Neuropsychopharmacology* 44(1):140–154. <https://doi.org/10.1038/s41386-018-0156-z>
36. Seibenhener ML, Wooten MC (2015) Use of the Open Field Maze to measure locomotor and anxiety-like behavior in mice. *J Vis Exp* 96:e52434. <https://doi.org/10.3791/52434>
37. Pan HQ, Zhang WH, Liao CZ, He Y, Xiao ZM, Qin X, Liu WZ, Wang N, Zou JX, Liu XX, Pan BX (2020) Chronic stress oppositely regulates tonic inhibition in Thy1-expressing and non-expressing neurons in amygdala. *Front Neurosci* 14:299. <https://doi.org/10.3389/fnins.2020.00299>

**Publisher's note** Springer Nature remains neutral with regard to jurisdictional claims in published maps and institutional affiliations.